DESIGN AND EXPERIMENT OF SEED-FILLING COMPONENT FOR RICE HOLE SEEDER
/
水稻穴播器取种装置设计与试验

Huyang TANG [1)], Gang WANG [1)], Bo ZHOU [1)], Yu WAN [1)], Fuming KUANG [1)], Wei XIONG [1)], Dequan ZHU [1)], Shun ZHANG *[1, 2)]

[1)] College of Engineering, Anhui Agricultural University, Hefei, Anhui, 230036, China
[2)] Engineering Laboratory of Intelligent Agricultural Machinery Equipment, Anhui, Hefei, 230036, China
Tel: +86 18856922971; E-mail addresses: shunzhang@ahau.edu.cn
DOI: https://doi.org/10.35633/inmateh-72-69

Keywords: *rice, film mulching, hole seeder, seed-filling component, DEM*

ABSTRACT
The core equipment of rice dry direct-seeding with film mulching devices shows poor adaptability to rice varieties, struggling to accommodate diverse seeding quantity for both hybrid and conventional rice varieties. A seed-filling component with unilateral and bilateral seed-filling function was designed to solve this challenge. Through theoretical analysis the key structural parameters of the seed-filling component were determined. Then Discrete Element Method (DEM) simulations were conducted to analyze the seeding performance, leading to the identification of optimal parameters for orifice width and orifice deflection angle of the seed-filling component, which are 7.7 to 8.5 mm and 1.71 to 2.41 degrees, respectively. Bench experiments using the central composite design indicates that the optimal parameters for the seed-filling component's orifice width and orifice deflection angle are 8.1 mm and 1.99 degrees, respectively. In the optimal combination of orifice parameters, for unilateral seed-filling in hybrid rice, the miss-seeding rate is 4%, the qualified rate is 84.8%, and the reseeding rate is 11.2%. For bilateral seed-filling in conventional rice, the miss-seeding rate is 4.2%, the qualified rate is 85.2%, and the reseeding rate is 10.6%. The result of field hole-seeding with film mulching is consistent with the result of indoor bench experiments, demonstrating that the seed-filling component of the hole seeder can meet the seeding requirements for rice precision direct-seeding with film mulching. This paper provides theoretical reference for the design and optimization of the seed-filling component for rice hole-seeding equipment.

摘要
针对水稻覆膜旱直播核心装备穴播器品种适应性差，难以兼用于穴播量迥异的杂交稻和常规稻覆膜播种的问题，设计了一种具有双侧充种功能的取种装置，理论分析确定了取种装置的关键结构参数，进行了排种性能的离散元EDEM仿真分析，明确了取种装置进种口宽度和型孔偏转角的取值范围，分别为7.7~8.5 mm和1.71～2.41°；中心组合试验设计方法的台架排种试验表明，最佳的取值装置进种口宽度和型孔偏转角分别为8.1 mm和1.99°，此时，单侧充种播种杂交稻，漏播率为4%、合格率为84.8%、重播率为11.2%，双侧充种播种常规稻，漏播率为4.2%、合格率为85.2%、重播率为10.6%，田间覆膜播种试验与室内台架排种试验结果一致，表明穴播器取种装置能满足水稻覆膜精量穴播的排种要求。本文为水稻穴播器取种装置的设计及优化提供理论参考依据。

INTRODUCTION
As one of the essential global cereal crops, rice holds a significant position within agricultural production. According to the statistics, in 2021, the worldwide rice cultivation area reached 160 million hectares, accounting for 10.7% of the total cultivated area for all crops, ranking only behind maize and wheat. The global rice production reached 750 million metric tons, constituting 16.8% of the total crop production (*World Food and Agriculture – Statistical Yearbook 2021*, *2021*).

Rice, known as a "water-loving crop", exhibits the highest water consumption among all crops, utilizing 25% of the global agricultural freshwater resources *(Liu et al., 2015; Tao et al., 2016*). The hole-seeding with film mulching for rice technology, achieved through surface mulching, not only reduces soil water evaporation and enhancing soil moisture retention capacity but also converts natural precipitation into effective rainfall and increases soil water storage. This approach can save 50% to 70% of irrigation water compared to conventional direct seeding methods (*Li H. et al., 2020; Sandhu et al., 2019*). In addition, traditional rice direct seeding is susceptible to the influence of weather and weed infestation (*Kakumanu et al., 2018; Singh et al., 2015*), especially during the early growth stages, which can lead to problems like poor seedling emergence or malnutrition in rice seedlings, ultimately resulting in reduced yields *(Ghosh et al., 2017*).

Film mulching not only suppresses weed growth but also raises the soil temperature on the surface, and creates a microclimate conducive to rice growth under the mulch. This microclimate ensures the necessary temperature and moisture for early seed germination, root growth, and plant development, ensuring emergence rates, survival rates and adequate nutrient supply, thereby reducing the risks associated with direct seeding of rice *(He et al., 2013; Li H. et al., 2021*). Rice seeding with film mulching can also promote soil organic carbon mineralization *(Guan et al., 2022; Yang et al., 2020*), increasing soil microbial populations, improving soil structure, enhancing enzyme activity, nutrient availability, and ultimately enhancing rice yields (*Hadden & Grelle, 2016*).

With the development of biodegradable films, the use of biodegradable properties to replace the non-degradable aspects of traditional films for rice dry direct seeding with film mulching, it's an effective means to achieve economically and environmentally friendly, which reduces costs and improves efficiency (*Yin et al., 2019*). This has become a significant driving force for the development of rice hole seeding with film mulching technology and equipment. However, suitable devices of rice mulch hole-seeding with film mulching are currently lacking. Niu Qi and others modified seed-filling component of cotton hole seeder for rice hole seeding with film mulching by using a shovel-shaped seed-filling component. But their design was relatively simple, and the seed-filling component was fixed. It required a brush to assist with the clearing of seeds. As a result, the seeding quantity couldn't be adjusted, and it couldn't accommodate the different seeding quantity requirements of various rice varieties (*Niu et al., 2016*). Hui Li used a mini shovel in combination with an independent hole seed-metering device to achieve rice hole-seeding on film. However, the structure was complex, and the seeding quantity was difficult to adjust (*Li H. et al., 2021*).

In response to the current challenge of rice mulch seeding machines that are not adaptable for seeding substantially different quantities for hybrid and conventional rice, this study aimed to design and experiment the seed-filling component. This component can be used for both unilateral and bilateral seeding, allowing for self-clearing. The goal was to achieve rice hole seeding with film mulching for various rice varieties with different seeding quantity, thus meeting the specific agronomic requirements of different rice varieties.

MATERIALS AND METHODS

Structure and working principle of hole seeder

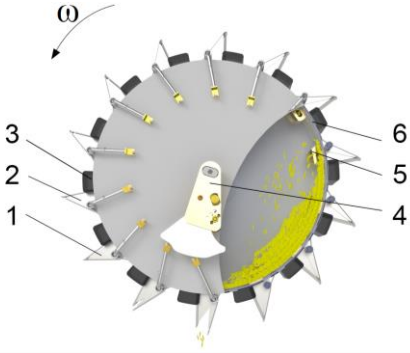

Fig. 1 - Schematic diagram of working principle of hole seeder

1. Seeding cylinder; 2. Duckbill; 3. Depth limit block; 4. Cam mechanism; 5. Seed-filling component; 6 Tile panel.

The hole seeder, is shown in Figure 1. During the seeding process, after seeds are loaded into the seed box, they descend by force of their dead weights into seeding cylinder. Positioned on bilateral of the seed-filling component secured to the tile panel are orifices. As the seeding cylinder advances through rotation, the seed-filling component undergoes synchronized rotation, causing rice seeds to be filled into it under the force of gravity lateral pressure from the surrounding rice seeds. The seed-filling component features a quantitative seed-filling space. The remaining quantitative rice seeds descend under the force of gravity, discharging the excess and re-entering the seeding cylinder. The remaining rice seeds within the seed-filling component proceed through a radial channel, entering the close state duckbill assembly as influenced by the rotational motion of the cylinder. Upon rotation of the rice-filled duckbill to its maximum soil depth, the moving duckbill, driven by the cam mechanism, opens fully and maintains this state for a specified interval. During this interval, the torsion spring accumulates energy, while the rice seeds inside the duckbill descend by gravity into the holes created by the duckbill's compression of the soil. This sequence completes the seeding process. Subsequently, as the duckbill fully disengages from the soil, the roller pendulum follower rotates to the cam's return phase. The release of energy from the torsion spring facilitates a smooth and controlled closure of the duckbill assembly.

Key parameters design of seed-filling component

The shapes and sizes of orifice inlet and outlet

As indicated in the literature (*Zhang, Li, et al., 2020*), rice seeds are filled into the orifice with their long axis aligned in the same direction as the tangential line of the seed-filling component's rotation. Based on the elliptical shape of the rice seeds, the orifice is designed to be elliptical, with its major axis aligned in the same direction as the tangential line of the rotating cylinder, as depicted in Figure 2.

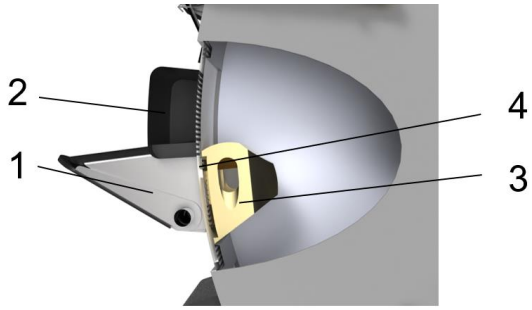

Fig. 2 - Single duckbill and seed pickup block connection diagram

1. Duckbill; 2. Depth limit block; 3. Seed-filling component; 4. Tile panel

The primary structural dimensions of the elliptical orifice are its length and width. Based on the seed-filling posture of the rice seeds, it is evident that within an equivalent range of dimensional variations, the rate per unit time seeds through the orifice is more sensitive to changes in the width dimension compared to the length dimension. Thus, the length dimension of the orifice only needs to accommodate the maximum length dimension of the rice seed, while the width dimension of the orifice must be determined experimentally based on the thickness dimension of the rice seed.

Considering the agronomic requirements of precision hole-seeding 5 to 10 seeds per hole for conventional rice, and in light of the characteristics of seed filling on bilateral of the seed-filling component, it is appropriate to fill 2 to 5 seeds on unilateral. Then the width dimension W of the orifice can be preliminarily determined within a design range using Equation (1).

$$3c_{\max} < W < 6c_{\min} \tag{1}$$

where: c is rice thickness size, mm.

To prevent rice seeds from mutually "crowding out" when entering the orifice, leading to arch, and to facilitate smooth entry of rice seeds into the radial channel of the orifice, the design of the seeds outlet is configured as a larger flow-rate square. Therefore, the orifice width and the side length of the seeds outlet should satisfy the following equation:

$$l > a_{\max} + c_{\max} \tag{2}$$

where: a is rice length size, mm; b is rice width size, mm; l is orifice width, mm.

The external dimensions of common rice seeds are summarized in Table 1 as follows:

Table 1

Rice seed outline size

Average triaxial size of rice seed (Length×Width×Thickness)	Maximum length size [mm]	Maximum width size [mm]	Maximum Thickness Size [mm]	Minimum Thickness Size [mm]
9.18×2.48×2.02	11.29	3.38	2.59	1.5

Based on Table 1 and the equations (1) and (2), the design values for the length of the orifice and side length of the seeds outlet are 14 mm. The appropriate width dimension for the orifice falls within the range of 7.7 to 8.5 mm.

Orifice deflection angle

As shown in Figure 3, by deviating the orifice at a certain angle in the opposite direction to the rotation of the seeding cylinder relative to the radial channel, the length of the orifice slope can be extended. Then the axial distance from the end face of the orifice to the vertical channel end face is reduced, contributing to the reduction of the axial dimension of the seed-filling component.

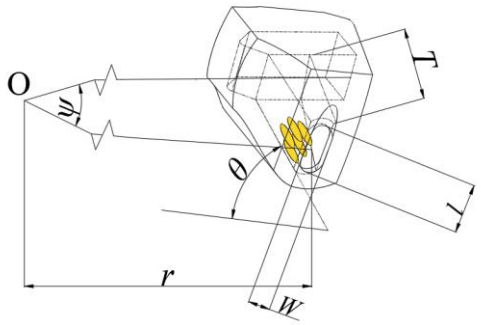

Fig. 3 - Illustration of the orifice deflection angle result

To ensure that rice seeds do not prematurely enter the radial channel during the filling and clearing phases, the value of the orifice slope angle θ needs to be determined based on the rice seed's friction angle. Theoretical analysis reveals that the orifice slope angle θ must be greater than the sliding friction angle of the rice seed. The geometric relationship between the orifice deflection angle ψ_1 and the orifice slope angle θ can be deduced from Figure 3.

$$\psi = \tan^{-1}\left(\frac{T}{\tan(0.5\pi-\theta)(r+0.5W)}\right) \tag{3}$$

where: r is distance from the geometry center of the orifice to the circle center of the seeding plate, mm; r is set to 188 mm; ψ is orifice deflection angle, (°); T is axial distance from the end face of the orifice inlet to the end face of the radial channel, mm. In this study, T is set to 9 mm.

As indicated in the literature (*Jun et al., 2021*) the coefficient of friction between rice seeds and ABS plastic is 0.5. To ensure that rice seeds does not prematurely slide into the channel during the filling phase of seed-filling component, the orifice slope angle θ should not be less than 30°. Therefore, when the orifice width is 8.1 mm, the curve of the orifice slope angle relative to the orifice deflection angle is illustrated in Figure 4:

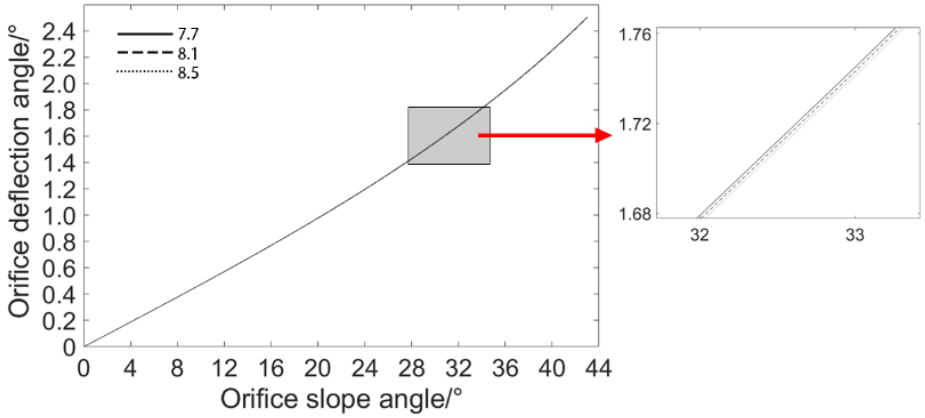

Fig. 4 - Relationship curve between orifice slope angle and orifice deflection angle

From Figure 4, it is evident that the orifice deflection angle ψ increases as the orifice slope angle θ increases. And the increase in orifice slope angle leads to a decrease in the internal seed-filling space within the orifice. Therefore, to fulfill the above requirements, the orifice deflection angle ψ should be greater than 1.60°.

Seeding performance simulation

Rice seed particle model

The experimental rice variety were selected from the conventional rice variety Huanghuazhan, which is widely grown in the lower-middle reaches of the Yangtze River in China. Based on the average triaxial dimensions of rice seeds by Huanghuazhan, and non-spherical particles modeling method based on EDEM software, multi-spherical composite approach is adopted, as illustrated in Figure 6. Since the width and thickness dimensions of rice seeds are relatively close, the width of the rice seed simulation particle is taken

as the average of the rice seed's average width and thickness dimensions, while the length of the particle is the average length dimension of the rice seed. As few filled spheres as possible were used to approximate the 3D model of the rice seed to minimize the simulation computation time.

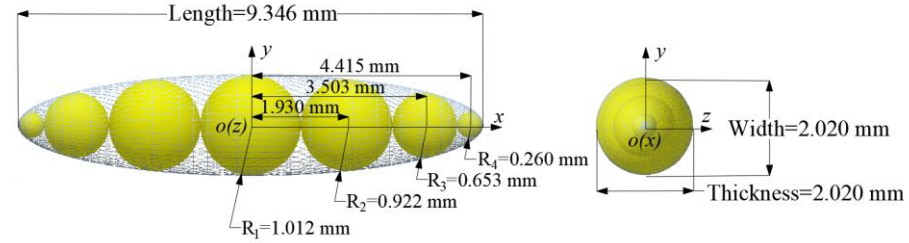

Fig. 6 - Rice seed particle model

Simulation model of hole seeding

Due to the multitude of components in the hole seeder, some of these components are not related to the seed filling process and the movement of seed particles within the seeding cylinder. To enhance simulation efficiency, the simplified hole seeder model is imported into EDEM 2022 software in STEP format. Based on the material characteristics of rice seeds and the actual materials of the hole seeder components, the material parameters for rice seed particles and each component are set, along with the contact parameters between particles and components *(Zhang, Tekeste et al., 2020)*.

The particle factory is situated within the cylinder, the particle generation method is Dynamic, the generation rate is 10000 particles/s, and the generation time is 0.2 s. Following the normal distribution characteristics of rice seed's triaxial dimensions, simulation particle sizes are set according to the standard normal distribution *(Li Y. & Xu, 2005*). As dry rice seeds have negligible adhesion forces on their surfaces, and weak electrostatic forces between the seeds are ignored, the Hertz-Mindlin no-slip contact model is selected for the simulation. The simulation model is depicted in Figure 7.

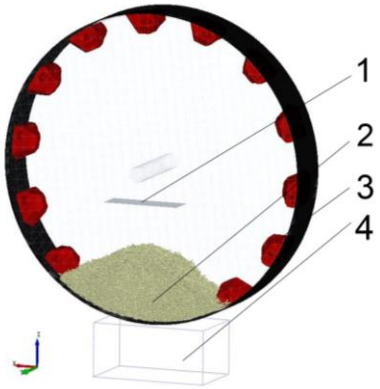

Fig. 7 - Simulation model of seeding device

1. Particle factory; 2. Rice seeds; 3. Seed-filling component; 4. Statistical unit of seed number per hole

Evaluation indicators

The experiment reference to the NY / T 987—2006 *(Standard for operating quality of hill-drop drill with film mulching*, 2006), the evaluation indicators for the hole seeder's performance are based on qualified rate, miss-seeding rate, and reseeding rate. To clarify the seed-filling pattern of seed-filling component and to avoid the influence of randomness in bilateral seed-filling on the assessment of seeding performance, considering the relatively independent unilateral seed-filling method of the seed-filling component, both simulation and bench experiment closed off unilateral orifice of the seed-filling component. This means that only the impact of unilateral seed-filling on the seed-filling component's performance is observed. Given that the recommended seeding range for conventional rice hole-seeding is 5 to 10 grains per hole, for unilateral seed filling, 2~5 seeds per hole is considered as qualified, less than 2 seeds per hole is considered as miss-seeding, and more than 5 seeds per hole is considered as reseeding. Therefore, the proportion of the total number of holes in the three results to the total number of holes in the experimental statistics is calculated, and the evaluation indexes were miss-seeding rate M (%), qualified rate Q (%), and reseeding rate R (%).

For the seeding performance simulation, a continuous count of 100 holes of rice seeds discharged by the hole seeder is taken as the experimental sample. In the bench experiment, a continuous count of 250 holes of rice seeds discharged by the hole seeder is taken as the experimental sample, and this process is repeated 2 times to account for the impact of the randomness in bench seeding on the experimental results.

Experiment design

To explore the effect of the orifice width and orifice deflection angle on the seeding performance, single factor seeding simulation tests were carried out separately. Under the condition of orifice deflection angle of 2.06°, the orifice width is set at 7.7, 7.9, 8.1, 8.3, and 8.5 mm, forming five levels.

To investigate the impact of the orifice deflection angle of the seed-filling component on the seeding performance, with an orifice of 8.1 mm, the orifice deflection angle is set at 1.60, 1.83, 2.06, 2.29, and 2.52°, forming five levels.

Bench experiment

Test materials and equipment

The experimental rice variety used was "Huanghuazhan". The experimental setup is illustrated in Figure 8. The hole seeder was driven by a direct current speed control motor (34CS85KF-490Z, Rayleigh Intelligent Technology Co., Ltd.), and a high-speed camera (i-SPEED 3 high-speed camera, Olympus Corporation, Japan) was used to count the number of seeds per hole.

Fig. 8 - Bench seeding experiment equipment

1. High-speed camera; 2. Hole seeder; 3. High-speed camera monitor; 4. Motor speed controller

Before the experiment, the high-speed camera lens was aligned with the duckbill open seeding position, and aperture and focal length were adjusted to ensure a clear view of the rice seeds being dispensed by the duckbill on the display screen. The shooting rate was set to 300 frames/s, and the resolution was set to 1280×1024. Continuous filming and recording captured the seeding situation in the seeding area when the hole seeder was stable. The recorded video was imported into the i-SPEED Suite software for frame-by-frame playback and the counting of seeding quantity per hole.

Referring to the generally operating speed of rice hole seeder with film mulching is between 0.5 to 1.2 m/s (*Jun et al., 2021*), the forward speed of cylinder is determined to be 0.8 m/s, and the rotational speed is 38 r/min.

Experimental design

In order to investigate the effects of the orifice width, orifice deflection angle, and their interaction on the seeding performance, and to determine the suitable parameter combinations, two factor central composite design was used. The levels of the factors were determined based on the single factor experiment results of seeding simulation. The experiment factors and their coded levels are presented in Table 3.

Table3

Experiment factor coding and level setting

Code	Orifice width *A*	Orifice deflection angle *B*
-1.414	7.8	1.71
-1	7.9	1.81
0	8.1	2.06
1	8.3	2.31
1.414	8.4	2.41

Field experiment

Experiment condition

To investigate field seeding performance of the hole seeder, a field experiment was conducted in June 2022 at Fenfang Village, Feixi County, Anhui Province, China. The hole seeder was assembled onto a rice hole-seeding with biodegradable film mulching machine and towed by the tractor. The experiment was carried out with reference to the *Standard for operating quality of grain film-cover hill-drop drill* NT/Y 987—2006. The forward speed of machine was set at 0.8 m/s on the field, consistent with the indoor bench experiment's operating speed of hole seeder.

After seeding, a random section of the experimental field, 20 meters in length, was selected for seed counting. Each row was continuously counted for 250 rice seeds, and this process was repeated for 8 rows. The aim was to calculate the miss-seeding rate, qualified seeding rate, and reseeding rate.

RESULTS

Analysis of seed filling process

As shown in Figure 10, this illustrates the s motion schematic of seed particles.

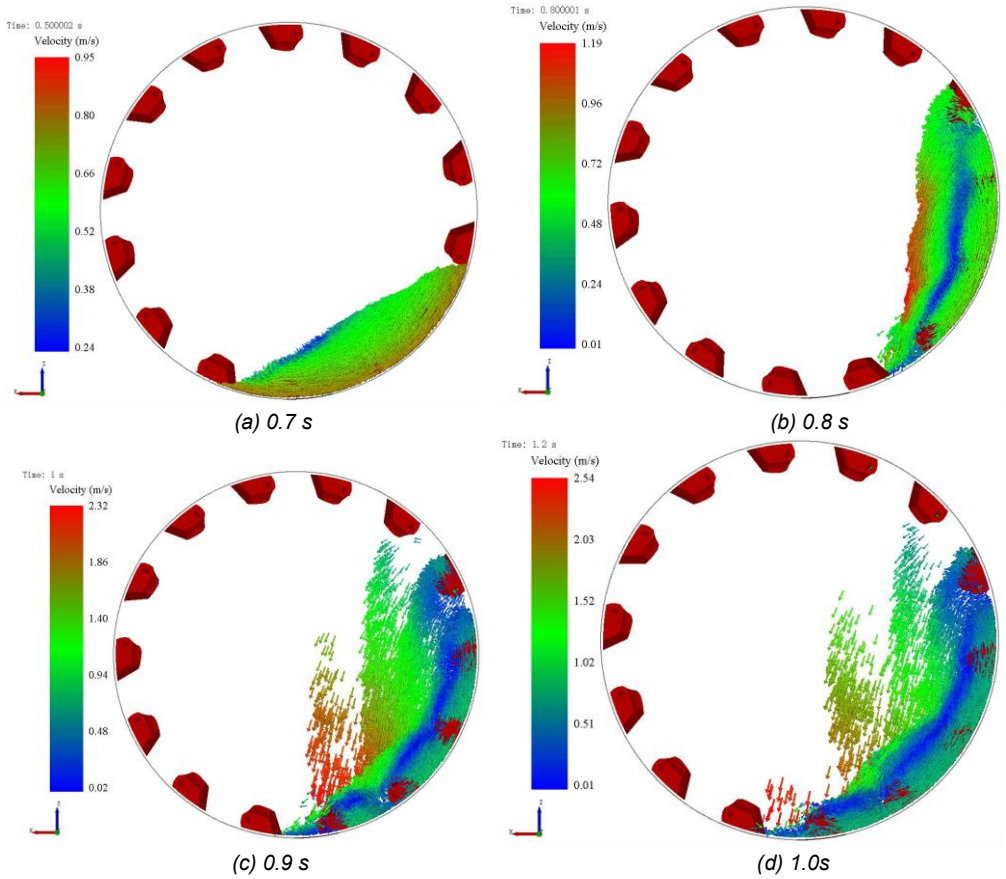

(a) 0.7 s *(b) 0.8 s*

(c) 0.9 s *(d) 1.0s*

Fig. 10 - Motion Schematic of seed particles

When seeding with the hole seeder, the particles movement process inside the seeding cylinder is shown in Figure 10, and red part represents the seed-filling component. After all the rice grain particles are generated and stabilized, the seeding cylinder begins to rotate. Driven by the seeding component and the friction of seeding cylinder's inner wall, the rice seeds move along with the cylinder, forming a semilunar shape region (Fig.10a). As the seeding cylinder continues to rotate, the semilunar seed particles are lifted to an approximate vertical state, and the surface layer of the seed particles is formed into a reflux zone under the action of gravity (Fig.10b).

As the seeding drum continues to rotate, the seeds at the top of seed-filling component slipped down followed one another, making the reflux zone increase (Fig.10c). When the hole seeder worked stably, the particles in the seeding cylinder formed three different motion regions: First, the particles close to the inner wall of the seeding cylinder rotated in synchronization with the seeding cylinder under the friction of the cylinder's inner wall and the pushing force of the seed-filling component; second, the rice seeds in the upper right area of the seed-filling component form small scattered local reflux zone; third, the reflux zone composed of the surface layer rice seeds and the refluent seeds carried away from the top of the seed-filling component (Fig.10d).

Figure 11 depicts the process of seed filling in the seed-filling component. The seed-filling component initially enters from the bottom of the seed particles (Fig.11a). As the seeding cylinder rotates, the rice seeds (in yellow) enter the seed-filling component through the orifice, approximately aligning their long axis with the tangential direction of the seed-filling component's rotation (Fig.11b). The rice seeds inside the orifice are poured onto the slope of the orifice under the influence of their self-gravity as the seed-filling component continues to rotate. Due to the limited seed-filling space of the orifice, when the slope can no longer accommodate more rice seeds pouring in, the excess rice seeds (in silver) will slide out of the orifice under the force of gravity. This achieves the self-clearing of rice seeds based on their dead weight. The quantified rice seeds poured onto the slope will continue to rotate with the seed-filling component and enter the radial channel through the seeds outlet.

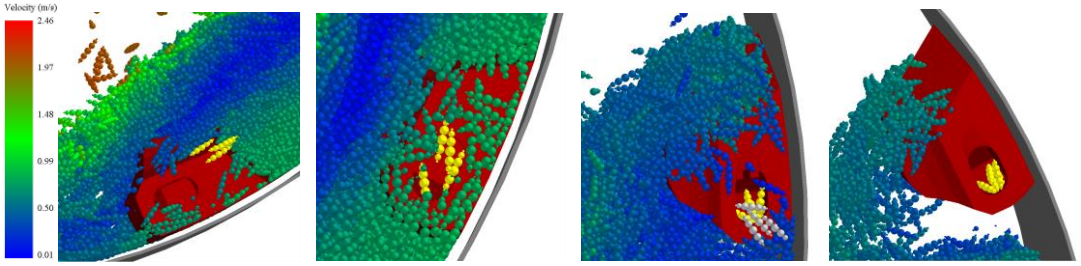

(a) (b) (c) (d)

Fig.11 - Schematic of seed filling process

Result and analysis of Central composite design

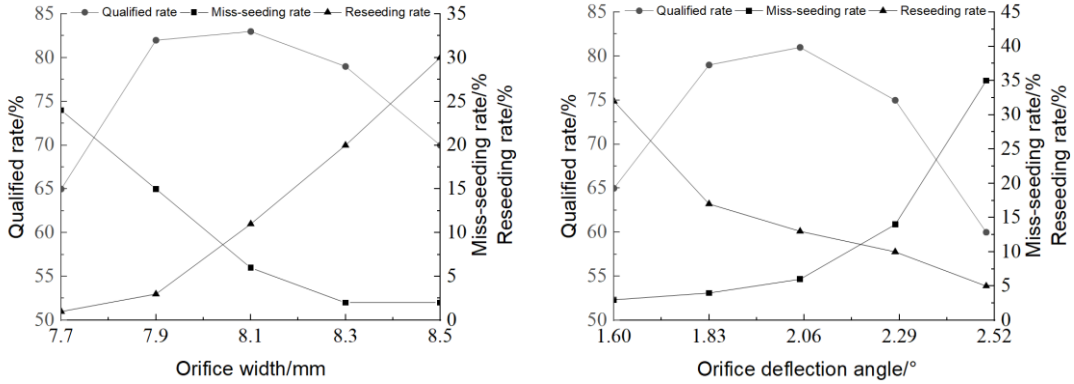

(a) (b)

Fig. 12 - Result of Central composite design

Influence of orifice width on seed filling performance are as shown in Figure 12(a), with the increase in the width of the orifice, the qualified rate of seed-filling process first increases and then decreases. The miss-seeding rate first decreases significantly and then decreases slowly, and the reseeding rate first increases slowly and then increases significantly. When the orifice width is too small, only a few rice seeds can be filled into the orifice as the seeding cylinder rotates, resulting in a high miss-seeding rate and low qualified rate and reseeding rate. As the orifice width gradually increases, multiple rice seed particles are more likely to enter the orifice, leading to a significant reduction in the miss-seeding rate and a substantial increase in the qualified rate, with a slight increase in the reseeding rate. When the orifice width becomes too large, an excessive number of rice seed particles enter the orifice, causing a further decrease in the miss-seeding rate, a significant increase in the reseeding rate, and a noticeable decrease in the qualified rate. It can be seen that the suitable orifice width should be in the range of 7.8 to 8.4 mm, at which point the qualified rate of seed-filling process is around 80%.

The experimental results of the influence of orifice width on seed filling performance, are shown in Figure 12(b). They reveal that with the increase in the orifice deflection angle, the qualified rate of seed-filling process initially increases and then decreases. The miss-seeding rate initially rises slowly and then increases rapidly, and the reseeding rate initially decreases rapidly and then decreases slowly. When the orifice deflection angle is too small, the internal seed-filling space of the orifice is relatively large, making it easier for multiple rice seed particles to lie flat on the slope inside the type hole, resulting in a low miss-seeding rate and a high reseeding rate. As the orifice deflection angle gradually increases, the internal seed-filling space of the orifice decreases, causing a slow increase in the miss-seeding rate, a substantial increase in the qualified rate, and a significant

decrease in the reseeding rate. When the orifice deflection angle becomes too large, the internal seed-filling space of the orifice is too small, and only a few rice seed particles enter the orifice, leading to a rapid increase in the miss-seeding rate, a certain decrease in the reseeding rate, and a noticeable decrease in the qualified rate. It can be seen that the suitable orifice deflection angle should be around 1.71 to 2.41 degrees, at which point the qualified rate of seed-filling process is approximately 75%.

Results and analysis of bench experiment of seeding performance

The results of the bench experiment are presented in Table 4.

Table 4

Experiment program and results of bench experiment

Experiment codes	Experiment factors		Evaluation indicators		
	X_1	X_2	M%	Q%	R%
1	7.9	1.81	4.8	78.4	16.8
2	8.3	1.81	2.2	77.6	20.2
3	7.9	2.31	6.2	81.8	12.0
4	8.3	2.31	5.2	75.6	19.2
5	7.8	2.06	6.0	83.6	10.4
6	8.4	2.06	2.4	76.4	21.2
7	8.1	1.71	1.8	78.8	19.4
8	8.1	2.41	6.2	80.2	13.6
9	8.1	2.06	4	83.4	12.6
10	8.1	2.06	4.3	84.2	11.5
11	8.1	2.06	4.4	84.0	11.6
12	8.1	2.06	4.8	85.2	10.0
13	8.1	2.06	4.2	84.6	11.2
14	8.1	2.06	4.2	84	11.8

Table 5

ANOVA table of bench test result

Source of Variance	M%				Q%				R%			
	SS	df	F	P	SS	df	F	P	SS	df	F	P
Model	24.23	5	24.83	**	137.99	5	31.09	**	203.22	5	37.35	**
X_1	9.44	1	48.37	**	36.90	1	41.57	**	83.68	1	76.89	**
X_2	14.10	1	72.26	**	1.43	1	1.61		24.51	1	22.52	**
X_1X_2	0.64	1	3.28		7.29	1	8.21		3.61	1	3.32	
X_1^2	0.03	1	0.17		44.93	1	50.62	**	42.54	1	39.08	**
X_2^2	0.00	1	0.04		54.50	1	61.40	**	55.85	1	51.31	**
Residual	1.59	8			7.10	8			8.71	8		
Lack of Fit	1.19	3	5.40	0.05	5.23	3	4.65	0.07	5.07	3	2.33	0.19
Error	0.40.	5			1.87	5			3.64	5		
Total	25.82	13			145.09	13			211.93	13		

Using Design-Expert 12 software, a regression analysis was conducted on the experimental data in Table 4 to establish quadratic regression models for the variables of miss-seeding rate, qualified rate, and reseeding rate with respect to orifice width and orifice deflection angle. The regression equations are as follows.

$$\begin{cases} M = 4.32 - 1.09A + 1.33B + 0.40AB + 0.06A^2 - 0.03B^2 \\ Q = 84.23 - 2.15A + 0.42B - 1.35AB - 2.47A^2 - 2.72B^2 \\ R = 11.45 + 3.23A - 1.75B + 0.95AB + 2.40A^2 + 2.75B^2 \end{cases} \quad (6)$$

The analysis of variance results for the experimental data in Table 4 are shown in Table 5. According to Table 5, the regression model for miss-seeding rate is significant, while the models for qualified rate and reseeding rate are highly significant. This indicates the effectiveness of the regression models for each performance evaluation indicators. The lack-of-fit terms for all regression models are not significant ($P > 0.05$), which means that there is no significant curvature lack of fit in the models. Furthermore, the determination coefficients (R^2) for each regression model are respectively 0.94, 0.95, and 0.96, which indicates that the regression model equations are highly reliable, showing a strong correlation between model predicted values and actual values. It implies that the experimental design is reasonable, and the model equations can be used for analysis and prediction of seeding performance.

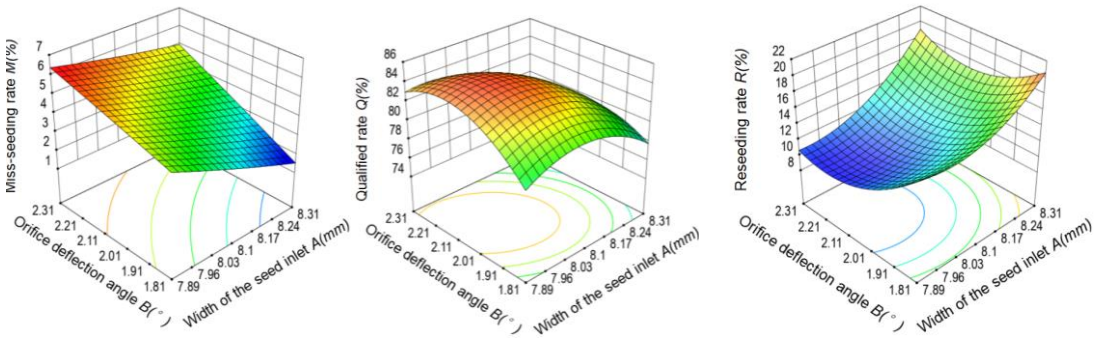

(a) Miss-seeding rate (b) Qualified rate (c) Reseeding rate

Fig. 14 - Influence of inlet width and hole deflection angle on test evaluation index

The response surface plots showing the influence of experimental factors on each evaluation indicators are presented in Figure 14. From Figure 14(a), it can be observed that when the orifice deflection angle is held constant, the miss-seeding rate decreases as the orifice width increases. Conversely, when the orifice width is held constant, the miss-seeding rate increases with the orifice deflection angle.

In Figure 14(b), it's evident that as both the orifice width and orifice deflection angle increase, the qualified rate initially rises and then declines. However, the variation in the qualified rate is more pronounced with changes in the orifice deflection angle, while changes in orifice width have a more moderate effect. This aligns with the variance analysis results, indicating that the orifice width significantly affects the qualified rate, while the influence of the orifice deflection angle is not significant. Figure 14(c) illustrates that when the orifice deflection angle is held constant, the reseeding rate first remains relatively stable and then increases rapidly as the orifice width widens. When the orifice width is constant, the reseeding rate first initially decreases and then rises with an increase in the orifice deflection angle.

Considering the changing trends of the evaluation indicators in Figure 14, it is necessary to carefully select the reasonable orifice width and orifice deflection angle to achieve a higher qualified rate and lower miss-seeding and reseeding rates.

Optimal combination of structure parameters

To obtain the optimal combination of structural parameters for the seed-filling component, achieving high qualified rate and low miss-seeding rate and reseeding rate within the range of experimental parameters, a multi-objective optimization model for the experiment structure parameters is established, as shown in Eq. (7):

$$\begin{cases} \min M(A,B) \\ \max Q(A,B) \\ \min R(A,B) \\ s.t 7.8 \le A \le 8.4 \\ 1.71 \le B \le 2.41 \end{cases} \quad (7)$$

The optimization model was solved using Design-Expert 12 software, resulting in orifice width of 8.1 mm and orifice deflection angle of 1.99°. At these optimized parameters, the seed-filling component exhibits the best seeding performance, with a miss-seeding rate of 3.95%, a qualified rate of 83.90%, and a reseeding rate of 12.15%. To verify the accuracy of the optimization results obtained, the seed-filling component with the optimized structural parameters was manufactured and subjected to bench experiments. In the unilateral seeding experiments, the results showed a miss-seeding rate of 4%, a qualified rate of 84.8%, and a reseeding rate of 11.2%. The errors in the corresponding evaluation criteria compared to the optimization results were all lower than 1%. This indicates that the validation experiment results align closely with the model predictions, further confirming the reliability of the regression model. The validation results also demonstrate that the seed-filling component with the optimized structural parameters, meets the seeding quantity requirements for hybrid rice precision direct-seeding with film mulching on unilateral seed filling process.

To meet the seeding quantity requirements for conventional rice precision direct-seeding with film mulching, the seed-filling component with the optimal structural parameters was used to conduct bilateral seeding bench experiments. The results showed a miss-seeding rate of 4.2%, a qualified rate of 85.2%, and a reseeding rate of 10.6%, which were similar to the seeding performance observed during bilateral seeding with the seed-filling component. This confirms that the designed approach of switching between bilateral and unilateral seeding to accommodate different varieties and seeding quantity is feasible.

Field experiment results

The results of field experiment are shown in Figure 15.

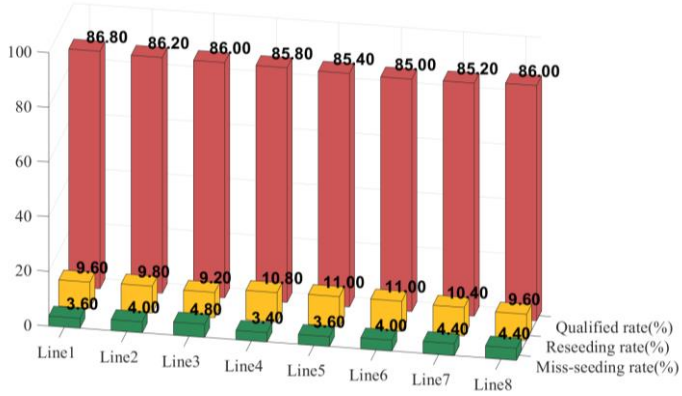

Fig. 15 - Field experiment performance test results

From Figure 15, it can be observed that the average qualified rate of each row for the field with hole seeder is 85.8%, the average miss-seeding rate is 4.03%, and the average reseeding rate is 10.17%. This indicates that the seed-filling component, which has the capability for bilateral seeding, can achieve stable seeding performance in the field and meet the seeding quantity requirements for rice precision direct-seeding with film mulching. However, in comparison to the results obtained from the beach seeding experiment, the field experiment shows a slightly lower miss-seeding rate and a slightly higher qualified rate. The reason for this difference could be attributed to the vibrations and bumps experienced by the field seeding equipment, which help seeds and the seed-filling component to exhibit relative sliding motion in the rotational direction, improving seeding performance, resulting in a reduction in miss-seeding rates, and an increase in the qualified rates. The field seeding scenario is shown in Figure 16.

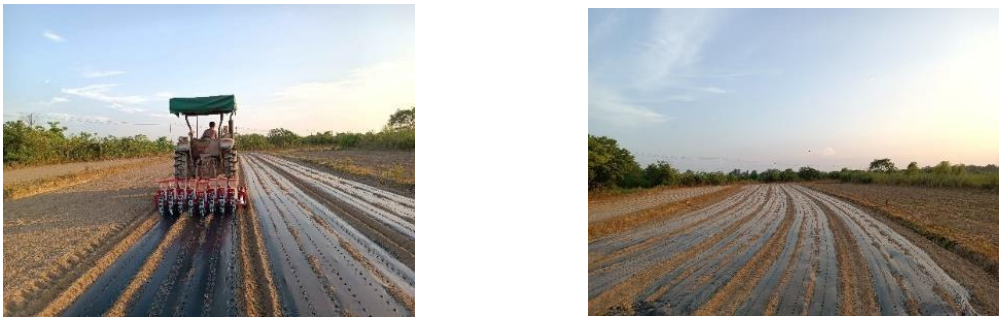

(a) Work scenario *(b) Sowing effect with biodegradable film mulching*

Fig. 16 - Field seeding experiment

CONCLUSIONS

(1) To meet the seeding quantity requirements for both hybrid rice and conventional rice, a seed-filling component with both unilateral and bilateral seeding capabilities was designed. The paper analyzed the key structural parameters of the seed-filling component based on the external characteristics of rice seeds and the quantitative seed filling method of the seed-filling component. It used DEM (Discrete Element Method) to simulate the seed-filling process of hole seeder. Single factor simulation experiment was conducted to investigate the effects of the orifice width and orifice deflection angle on the seed-filling performance. This helped determine the appropriate range of values for the key structural parameters.

(2) Central composite design between orifice width and orifice deflection angle was conducted. By using the multi-objective optimization model, the optimal structural parameter combination was determined, which consisted of an orifice width of 8.1 mm and an orifice deflection angle of 1.99°. Under this parameter combination, the unilateral seeding with the seed-filling component achieved a miss-seeding rate of 4%, a qualified rate of 84.8%, and a reseeding rate of 11.2% for hybrid rice. For conventional rice, the bilateral seeding experiments resulted in a miss-seeding rate of 4.2%, a qualified rate of 85.2%, and a reseeding rate of 10.6%, all meeting the seeding quantity requirements for rice direct-seeding with film mulching. Field seeding experiment demonstrated that the hole seeder equipped with seed-filling component had stable seeding performance.

ACKNOWLEDGEMENT

This work was supported by the National Natural Science Foundation of China, China (Grant numbers 51805005), Major Project of Natural Science Research in Universities of Anhui Province (Grant numbers KJ2021ZD0012), Key research and Development Project of Anhui Province (Grant numbers 202204c06020024) and Key programs of outstanding young talents in universities (Grant numbers gxyqZD2022016)

REFERENCES

Ghosh, D., Singh, U. P., Brahmachari, K., Singh, N. K., & Das, A. (2017). An integrated approach to weed management practices in direct-seeded rice under zero-tilled rice–wheat cropping system. *International Journal of Pest Management*, *63*(1), 37–46. https://doi.org/10.1080/09670874.2016.1213460

Guan, Z.-H., Wang, L., Turner, N. C., & Li, X. G. (2022). Plastic-film mulch affects partitioning of maize biomass and nutrients to grain. *Crop Science*, *62*(1), 315–325. https://doi.org/10.1002/csc2.20677

Hadden, D., & Grelle, A. (2016). Changing temperature response of respiration turns boreal forest from carbon sink into carbon source. *Agricultural and Forest Meteorology*, *223*, 30–38. https://doi.org/10.1016/j.agrformet.2016.03.020

He, H., Ma, F., Yang, R., Chen, L., Jia, B., Cui, J., Fan, H., Wang, X., & Li, L. (2013). Rice Performance and Water Use Efficiency under Plastic Mulching with Drip Irrigation. *PLoS ONE*, *8*(12), e83103. https://doi.org/10.1371/journal.pone.0083103

Jun, L., Dequan, Z., Qilei, T., Congyang, Y., Tingjue, W., Kang, X., Shun, Z., & Juan, L. (2021). Design and experiment of adjustable socket-wheel precision fertilizer apparatus for dry direct-seeding rice. *INMATEH-Agricultural Engineering*, *63*(1). https://doi.org/10.356.33/inmateh-63-12

Kakumanu, K. R., Kotapati, G. R., Nagothu, U. S., Kuppanan, P., & Kallam, S. R. (2018). Adaptation to climate change and variability: A case of direct seeded rice in Andhra Pradesh, India. *Journal of Water and Climate Change*, *10*(2), 419–430. https://doi.org/10.2166/wcc.2018.141

Li, H., Zeng, S., Luo, X., Fang, L., Liang, Z., & Yang, W. (2021). Design, DEM Simulation, and Field Experiments of a Novel Precision Seeder for Dry Direct-Seeded Rice with Film Mulching. *Agriculture*, *11*(5), 378. https://doi.org/10.3390/agriculture11050378

Li, H., Zeng, S., Luo, X. W., Zang, Y., Liang, Z. H., Li, X. L., Teng, S. Z., & Yang, W. W. (2020). Effects of degradable mulching film on soil temperature, seed germination and seedling growth of direct-seeded rice (ORYZA SATIVA L.). *Applied Ecology and Environmental Research*, *18*(6), 8233–8249. https://doi.org/10.15666/aeer/1806_82338249

Li Y., & Xu Y. (2005). Discrete Element Simulation on Particle Piling. *Journal of Agricultural Mechanization Research*, *2*, 57–59.

Liu, H., Hussain, S., Zheng, M., Peng, S., Huang, J., Cui, K., & Nie, L. (2015). Dry direct-seeded rice as an alternative to transplanted-flooded rice in Central China. *Agronomy for Sustainable Development*, *35*(1), 285–294. https://doi.org/10.1007/s13593-014-0239-0

Liu H., Su H., Li J., & Liu Z. (2019). Interactive Optimal Design System of Drum-type No-till Planter Mechanism. *Transactions of the Chinese Society for Agricultural Machinery*, *50*(3), 58–68.

Liu H., Wen H., Gai G., & Tang S. (2017). Design and Experiment on Passive Drum-type No-till Planter Cavitation Mechanism. *Transactions of the Chinese Society for Agricultural Machinery*, *48*(9), 53–61.

Niu Q., Wang S., & Chen X. (2016). Design of Rice Planter with Plastic Film Mulched Drip Irrigation. *Transactions of the Chinese Society for Agricultural Machinery*, *47*(S1), 90-95+102.

Sandhu, N., Subedi, S. R., Singh, V. K., Sinha, P., Kumar, S., Singh, S. P., Ghimire, S. K., Pandey, M., Yadaw, R. B., Varshney, R. K., & Kumar, A. (2019). Deciphering the genetic basis of root morphology, nutrient uptake, yield, and yield-related traits in rice under dry direct-seeded cultivation systems. *Scientific Reports*, *9*(1), Article 1. https://doi.org/10.1038/s41598-019-45770-3

Singh, M., Bhullar, M. S., & Chauhan, B. S. (2015). Influence of tillage, cover cropping, and herbicides on weeds and productivity of dry direct-seeded rice. *Soil and Tillage Research*, *147*, 39–49. https://doi.org/10.1016/j.agwat.2019.02.004

Tao, Y., Chen, Q., Peng, S., Wang, W., & Nie, L. (2016). Lower global warming potential and higher yield of wet direct-seeded rice in Central China. *Agronomy for Sustainable Development*, *36*(2), 24. https://doi.org/10.1007/s13593-016-0361-2

Yang, X., Liu, H., Mao, X., Deng, J., & Haefele, S. M. (2020). Non-flooding rice yield response to straw biochar and controlled-release fertilizer. *Agronomy Journal*, *112*(6), 4799–4809.

https://doi.org/10.1002/agj2.20430

Yin, M., Li, Y., Fang, H., & Chen, P. (2019). Biodegradable mulching film with an optimum degradation rate improves soil environment and enhances maize growth. *Agricultural Water Management*, *216*, 127–137. https://doi.org/10.1016/j.agwat.2019.02.004

Zhang S., Li Y., Wang H., Liao J., Li Z., & Zhu D. (2020). Design and Experiment of U-shaped Cavity Type Precision Hill-drop Seed-metering Device for rice. *Transactions of the Chinese Society for Agricultural Machinery*, *51*(10), 98–108.

Zhang, S., Tekeste, M. Z., Li, Y., Gaul, A., Zhu, D., & Liao, J. (2020). Scaled-up rice grain modelling for DEM calibration and the validation of hopper flow. *Biosystems Engineering*, *194*, 196–212. https://doi.org/10.1016/j.biosystemseng.2020.03.018

*** *World Food and Agriculture – Statistical Yearbook 2021.* (2021). *FAO.* https://doi.org/10.4060/cb4477en

*** *NT/Y 987—2006. (2006). Standard for operating quality of hill-drop drill with film mulching* (铺膜穴播机行业标准). National Standard of the People's Republic of China. (in Chinese)